Nucleation and growth of sodium chloride in confined geometries

J. Desarnaud[1*], H. Derluyn[2], J. Carmeliet[2], D. Bonn[1] and N. Shahidzadeh[1]
[1]Van der Waals-Zeeman Institute, Institute of Physics, University of Amsterdam, The Netherlands
[2]ETH, Institut für Technologie in der Architektur, Zürich Hönggerberg, Switzerland
* j.e.desarnaud@uva.nl

Abstract

Experiments on evaporation of aqueous sodium chloride solutions from micro capillaries demonstrate for the first time that there is a metastability limit to the solubility of NaCl. The supersaturation of the solution reached at the onset of crystallization is found to be very high, almost twice the saturation concentration. At this concentration, we observe a peculiar form of crystal growth: the very rapid growth of a single Hopper crystal in which many crystallites grow outwards from a single central nucleus. The high supersaturations achieved at the onset of crystal growth are found to be independent of the size, shape and surface properties of the micro capillary.

Keywords: metastability limit, NaCl, supersaturation, salt damage

1 Introduction

Nucleation and crystallization in porous media are very important subjects in different fields such as the semiconductor industry, oil recovery, soils mechanics, purification of pharmaceuticals and proteins [1-4]. There are also many direct applications, biomineralization [5], CO_2 sequestration where NaCl crystals that precipitate can completely block the porous medium in which the CO_2 should be injected [6,7]. For civil engineering, geology and conservation of cultural heritage, frost [8-9] and salt crystallization is one of the major cause of mechanical and physical weathering leading to the disintegration of rocks and building materials [10-14], and its influence is expected to increase due to global climate change [15].

In practice, the precise conditions under which the salt crystals nucleate and grow are very important but still unknown. The existence of a supersaturation in the salt solutions can account for an excess pressure exerted by the salt crystals against the pore walls (crystallization pressure) [16, 17] and hence damage the stone. In fact, any crystallization in solution process consists of two major steps: crystal nucleation and growth. The rate of nucleation and the growth speed are driven by the supersaturation ($\Delta\mu$) of the solution, since the latter is the driving force of both processes

$$\Delta\mu = \mu_s - \mu_c \approx \nu RT \ln S \qquad (1)$$

where μ_s and μ_c are the chemical potentials of a molecule in solution and in the bulk of the crystal phase, respectively; k is the Boltzmann constant, T is the absolute temperature and S is the relative supersaturation defined as ($S=C/C_{sat}$ with C concentration of the solution and C_{sat} concentration of the solution at saturation).

For a given supersaturation, by taking into account the non-ideal behaviour of the liquid phase, the total number of ions present and the interactions, the crystallization pressure due to the crystal growth may be expressed as [16]:

$$\Delta P = \frac{\nu RT}{V_m}\left(\ln\frac{C}{C_0} + \ln\frac{\gamma_{\pm}}{\gamma_{\pm,0}} + \frac{\nu_0}{\nu}\ln\frac{a_w}{a_{w0}}\right) \qquad (2)$$

where ν is the total number of ions per dissolved molecule (2 for NaCl) and V_m the molar volume of the crystalline phase. The first term in the parenthesis describes the supersaturation in terms of concentration, the second and third terms describe the no ideal behaviour of the concentrated salt solutions.

But this mechanism cannot explain all the degradations observed. It does not consider the influence of surface properties of the materials itself on the salt nucleation and crystallization even if it is well known that the intensity of damage depends on the quantity of salt as well as the characteristics of the porous network and the pore geometry. Indeed, a stone is a porous material composed of a network of angular pores of different sizes and shapes. Taber [18], Everett and [9] Scherer [12] claim that damaging stresses are expected only if the crystallization takes place in small pores because the salt solution constrained in fine pores could maintain a higher supersaturation [19-21]. It is also well established that the surface chemistry, the morphology and the shape of the surface play a crucial role in the nucleation [22-26].

New studies have shown that the kinetics of salts crystallization play an important role in the degradation [27,28]. It is clear that when the salts crystallize within the stone (a phenomenon called subflorescence) the decay is strong, harmful for the stone and a loss of material can be observed (i.e flaking and scaling).

Consequently a detailed understanding of how crystals nucleate and grow within porous media and lead to damage is needed.

In this study we have investigated at the microscale the role played by the nature, shape and size of the porous media on the kinetics of nucleation and growth of sodium chloride. Then, at the macroscale the damage process on Prague sandstone when the NaCl-solution is entrapped inside the stone and the salt crystallizes as subflorescence is studied.

2 Experimental section

At a microscale, using a phase contrast microscopy and direct imaging we have investigated the drying of a NaCl-solution in glass capillaries which are considered as simple model for a single pore in a porous medium. Different sizes of microcapillaries have been used (50 to 2000µm) and chemically different surfaces: hydrophobic (silanised: treated with OCTEO (Octyltrietoxysilane)) and hydrophilic (cleaned) [29]. The geometry of the microcapillaries is also changed; besides cylindrical we also use rectangular shapes since in real porous media liquid can be trapped within corners of the porous network [24, 30-32]. We study situations with slow evaporation (and consequently no large salt concentration gradients) by choosing the initial concentration in such a way that the surface tension and the contact angle of the salt solution were high enough to avoid the formation of wetting films. This corresponds to the most harmful situation where the solution cannot reach the surface of a porous medium like stone (because of the presence of a treatment product: water repellent, consolidant, anti-graffiti, wax, etc) [33] or very high concentration of salt solution or finally because of extreme conditions of drying [24] and the salts will crystallize as subflorescence.

Because the NaCl-solution evaporates and concentrates during the experiment, we measured the variations of the surface tension and the contact angles of the NaCl-solution on glass with regards to the salt concentration with an Easy-Drop device. The initial salt solutions (molar concentrations from 0,616 to 6,160 M) were prepared by dissolving NaCl (Sigma-Aldrich purity 99.9%) in Millipore water.

All experiments have been done in well controlled relative humidity (RH in a range from 2% to 68% ± 0.5%) and temperature (T =22°± 2°C)

A known volume (V_0) of the solution is introduced into the capillary and placed into a miniature climatic chamber with dimensions 1.5x2x6 cm^3 [27] under a microscope. By fixing the relative humidity of the ambient air in the climatic chamber [27], the evaporation rate of the solution is controlled. The volume change during the evaporation of the solutions inside the microcapillaries is subsequently followed by recording the displacement of the two menisci while simultaneously visualizing the onset of crystal growth in the solution directly with the optical microscope (Leica IDRM) coupled to a CCD camera.

At macroscale we investigated the crystallization of sodium chloride as subflorescence inside Prague Sandstone (porosity $\Phi \approx 29\%$, pore diameter dp ≈ 25 µm [34]) using scanning electron microscope (SEM, HITACHI TM 3000). To avoid the formation of efflorescence, the upper face of the sandstone samples (5x5x10mm) were treated with a consolidant (@)funcosil) and the 4 lateral faces were covered with parafilm. Then, the samples were impregnated with NaCl-solution by capillarity with an initial concentration of 4.9 M and left to dry in a homemade climatic chamber in which both temperature and humidity are imposed at T ≈ 22 ± 2°C and RH~50±2%.

3 Results and Discussion

3.1 Microscale experiments

The liquid/vapor surface tension (γ_{lv}) of the NaCl solution and its contact angle on glass slide (θ) increase linearly with the NaCl concentration (Figure 1). Using this relation, we define a critical salt concentration (S =4.47 M, i.e S = C/C_{sat}=0.72) above which the formation of wetting films in the edges of the square geometry is avoided [30] (the critical angle defined as $\theta c=\pi/N$ with N the number of sides, $\theta c = 45°$). The solution will be trapped inside the capillary without any connection with the entrance, and the crystallization will happen within it.

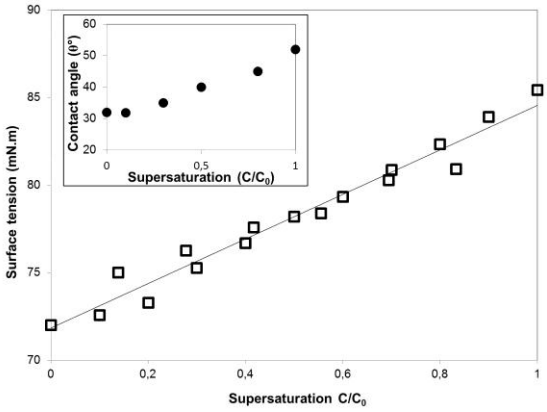

Figure 1: Linear increase of the surface tension of a NaCl-solution with regards to the supersaturation (C/C_{sat} with C concentration of the solution and C_{sat} concentration at saturation). In the frame, the contact angle θ of the NaCl-solution as a function of the supersaturation of the solution is plotted. (T ≈ 22.0 ± 0.5°C and RH~50±2%)

With regards to these results, we investigated the drying kinetics of 0.1 µl of NaCl-solution with an initial concentration of 4.9M (above the critical salt concentration) in the different capillaries.

As we expected no wetting films are observed in these experiments. The concentration for which nucleation is observed is constant and independent of the size, the shape of the microcapillary and the evaporation rate of the solution, the latter being controlled by the relative humidity (Figure 2). From more than 100 experiments, a supersaturation S of 1.6 ± 0.2 is calculated at the onset of crystallization ($S=C/C_{sat}$, with C the solution concentration at the moment when the crystallization occurs) (Figure 2).

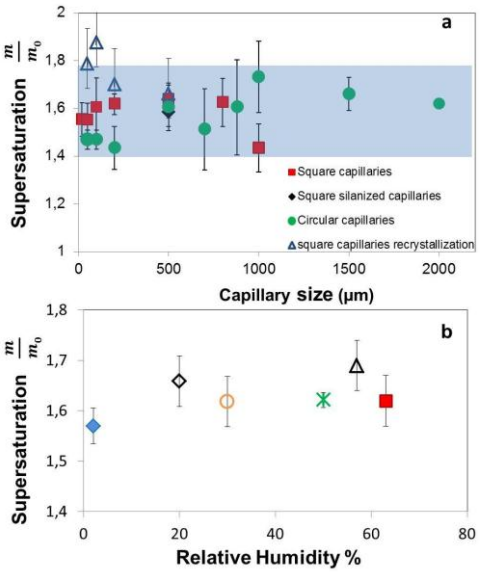

Figure 2: Supersaturation ($S = m/m_0$) of NaCl solutions reached by evaporation under isothermal conditions (22.0 ± 0.5°C) in various confined geometries and situations. (a) Data for microcapillaries of different sizes (from 20 to 2000 µm, i.e. below and above the capillary length), with two geometries (square and circular) and with different wetting properties (hydrophilic and hydrophobic). Recrystallization was studied after complete deliquescence of salt crystals. All measurements were done at a relative humidity (RH) of 52 ± 2%. (b) Data for 200 µm square capillaries at different evaporation rates (RH ranging from 2 to 68%) at the onset of spontaneous crystallization.

To assess the effect of impurities on the concentration for which nucleation is first observed, recrystallization experiments were conducted by performing repeated cycles of complete deliquescence (dissolution by water vapour) of the salt crystals followed by drying, a procedure that is known to efficiently expel impurities [25,27]. Our results show again that the value of 1.6 of supersaturation at the onset of crystallization is not affected within the experimental uncertainty (Figure 2a). One consequence of the evaporation is that, when the ion transport in the liquid phase is slower than the evaporation rate, there may be concentration gradients in the salt solution. This leads to a higher concentration of ions close to the meniscus, where the evaporation takes place. To see whether our limit of metastability is well defined in terms of NaCl concentration we calculated the Peclet number (Pe), which is a measure of the heterogeneity of the ion distribution. Pe is defined as the ratio between the convective and the diffusive transport of ions in the solution and can be calculated from various parameters such as the time-dependent NaCl

diffusion coefficient and the characteristic time of the displacement of the meniscus: Pe ≈ t_{diff}/t_s [30]. These can be calculated from $t_{diff} \approx z_0^2/D_{NaCl}(t)$ and $t_s \approx z_0/(dz/dt)$, with z_0 the initial meniscus position, z the position at the time t, and $D_{NaCl}(t)$ the diffusion coefficient at time t, which depends on the concentration and viscosity of the solution [30].

We find that at the start of the evaporation, Pe is of order unity at low relative humidity and in small microcapillaries, reflecting a rather heterogeneous distribution of ions in the solution (figure 3). However, the increase of the solute concentration in time leads to both a lower evaporation rate and a higher viscosity [35], reflected in a decrease of Pe. At the onset of crystallization, Pe reaches values on the order of 10-2 to 10-3 revealing that the ions are very homogeneously distributed in the solution and the limit of metastability is well defined.

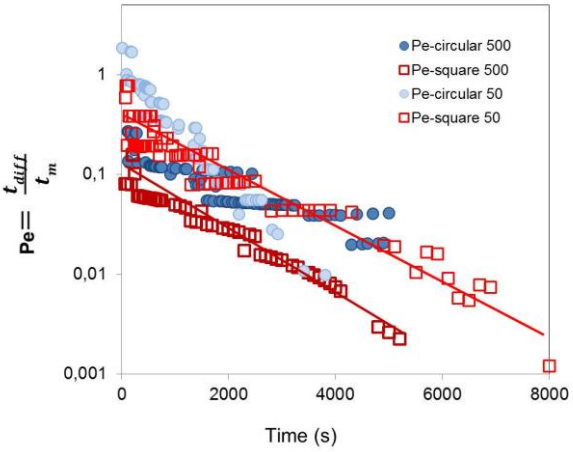

Figure 3: Peclet number *Pe* calculated at the meniscus as a function of evaporation time in square and circular capillaries with a size of 50 and 500 µm at RH = 52±2% and T = 22.0±0.5°C. The straight lines are guides to the eye.

From classical nucleation theories, one would also expect the probability of nucleation increase with time for which the solution has been supersaturated [36]. However the results as a function of the relative humidity show that the nucleation is only observed when a concentration of 1.6 ± 0.2 is achieved, independently of the time necessary to reach it. In our experiment, the necessary time to reach the limit of metastability strongly depends on the relative humidity and varies over more than an order of magnitude (figure 4).

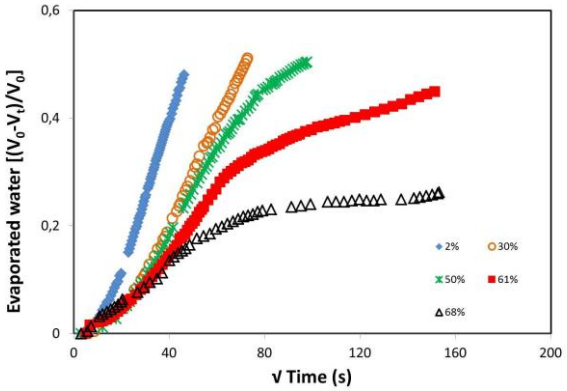

Figure 4: Normalized evaporated water volume from a 4.9M NaCl solution in 200 µm square capillaries as a function of time at different relative humidities (ranging from 2 to 68%) until spontaneous growth is observed. At an RH of 68% no crystals were formed. All measurements were done at T = 22.0±0.5°C

As can be observed in figure 4, the evaporation rate decreases in time but does not follow a $\sqrt{t}$ scaling as it would be for a simple diffusive process [37]. In fact, when the evaporation rate *e* is limited by diffusive vapor transport through the gas phase, it follows $e \approx \rho_g D \frac{(c_i - c_\infty)}{\delta}$ with ρ_g the vapor density, *D* the diffusion coefficient of water vapor through the gas, c_∞ the controlled water vapour concentration of the climatic chamber and c_i the water vapor concentration just above the menisci; δ is the characteristic distance over which diffusion takes place [30,36]. The drying rate is consequently controlled by δ and $c_i - c_\infty$; during the evaporation, $c_i - c_\infty$ decreases because the saturated vapor concentration decreases when the salt solution becomes more concentrated ($c_i / c_{pure\ water}$= 1-0.24 S) [38]; on the other hand δ is roughly the distance between the meniscus and the outlet of the capillary, which increases: both effects then lead to a decrease in evaporation rate, consequently a simple diffusive $\sqrt{t}$ scaling is not expected [36].

As a consequence, for humidities higher than 61%, corresponding to the equilibrium water vapour concentration above a solution close to S~1.6, the evaporation rate goes to zero as soon as $c_i = c_\infty$ (see e.g. the black symbols in Figure 4). Here, although the solution is supersaturated, no nucleation is observed because the value of 1.6 is not reached. In the experiments performed at humidities higher than 68 %, crystals no longer precipitate, since the evaporation stops until a perturbation is imposed to the system (i.e. rapid decrease of the temperature or relative humidity). This independently provides another value for the onset of nucleation: S = 1.60 ± 0.07 (Figure 2b), in agreement with the findings above.

It is worthwhile noting here that the time delay between the actual nucleation and our first observation of the crystal is given by its growth rate, which is typically in the order of a few (~5) μm/s for the cubic NaCl crystal [27]. This means that within a few seconds of its formation, the crystal is consequently observable. This results in an error on the supersaturation that is negligible, since the evaporation takes place over several hours. Moreover, any crystallization in the solution would change the equilibrium water vapor pressure above the solution and consequently the evaporation rate; we only notice such a change once the crystal is observed.

Since the nucleation appears to be homogeneous, Classical Nucleation Theory (CNT) can be used to predict the rate of crystal nucleation for sodium chloride as a function of the supersaturation. According to CNT, the rate of nucleation per unit volume can be calculated as the product of an exponential factor and a kinetic pre-factor [39,40]:

$$J = \kappa \, exp\left(-\frac{\Delta G^*}{kT}\right) \quad (3)$$

In the exponential factor, ΔG^* is the free energy cost of creating a critical nucleus and kT the thermal energy. The total Gibbs free–energy cost to form a spherical crystallite has a bulk and a surface term and can be expressed as:

$$\Delta G = \frac{4}{3}\pi R^3 \rho_s \Delta\mu + 4\pi R^2 \gamma \quad (4)$$

With ρ_s is the number density of the solid, $\Delta\mu$ the difference in chemical potential of the solid and the liquid and $\boldsymbol{\gamma}$ is the interfacial tension of the NaCl crystal with the solution (γ_{lc}~ 0.08 N.m^{-1} [39,40]). Here, the difference in chemical potential of the solid and the liquid, can be written in terms of the mean ionic activity of the solute a± [16,36], as:

$$\frac{\mu_l - \mu_c}{RT} = \nu \ln\left(\frac{a_\pm}{a_{0\pm}}\right) = \nu \, ln\left(\frac{\gamma_\pm}{\gamma_{\pm 0}}\frac{m}{m_0}\right) \quad (5)$$

where m and m_0 are the molalities at crystallization and equilibrium (mol.kg^{-1}) and $\gamma_\pm$ is the corresponding mean ionic activity coefficient and ν the sum of ions (2 for NaCl).

The energy of the critical nucleus ΔG^* is then:

$$\Delta G^* = \frac{4\pi}{3}\gamma R_c^{*2} \quad \text{with } R_c^* = \frac{2\gamma}{\nu\, kT ln\left(\frac{\gamma_{\pm}\, cm}{\gamma_{\pm 0} m_0}\right)} \qquad (6)$$

The kinetic pre-factor κ, which relates to the efficiency with which collisions between supernatant ions and the crystal interface produce crystal growth and is determined from $\kappa=\rho jZ$, where ρ is the number density of molecules in the liquid phase, Z the Zeldovich factor : $Z \approx 1/(n^*)^{2/3}$ with n* the excess number of molecules in the critical nucleus and *j* the rate at which molecules attach to the nucleus causing its growth. *j* is approximated as $j \sim \rho D R^*$ with D the diffusion constant of the molecules and R_c^* the radius of the critical nucleus [40].

The rate of nucleation J (m-3s-1) is plotted as a function of the supersaturation in Figure 5. It can be noticed that for supersaturation values lower than ~1.6 the nucleation rate is extremely small while very large in case of higher values. At S~1.6 the rate of the nucleation of sodium chloride is found to be 0.004 m-3s-1, which roughly corresponds to one nucleus in a typical volume considered here within our experimental time window (typically 5000 s). Moreover, the variation of the experimental parameters here (volume V, relative humidity etc.) does not significantly change the value of S~1.6 for which the nucleation becomes observable. Simply said, the nucleation rate depends so steeply on the supersaturation that all other parameters are irrelevant, in excellent agreement with all our observations.

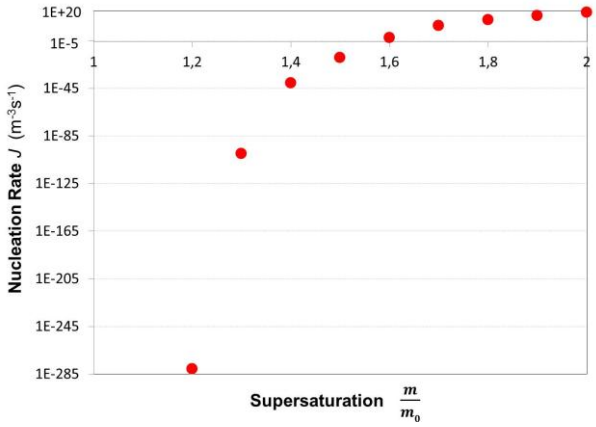

Figure 5: Nucleation rate J ($m^{-3}s^{-1}$) as a function of supersaturation $S=m/m_0$ of the solution calculated using equation (3)

Very recent simulations on NaCl solutions show surprisingly that already at a relatively low supersaturation, nucleation can be observed in smaller

system than ours on the time scale of a simulation [41,42] which is shorter than our experimental time. This discrepancy could be related to restrictions of the model used for the simulations or due to a difference in theoretical parameters (attempt frequency, dielectric constant, chemical potential difference and surface tension) compared to the experimental ones. For example, the solubility of NaCl is under estimated in the simulations compared to the real value; this seems an interesting item for further investigations.

Another very interesting observation is that at the onset of crystallization a single nucleus is observed to be growing very rapidly with a peculiar shape: a Hopper (skeletal) crystal (figure 6a,b). Such a hopper shaped crystal appears at high supersaturation because of the so-called “Berg-Effect” (on a flat surface, there is an excess of supersaturation near the edges) [43]. A new growth layer will be generated by the 2D nucleation near the edges and then the growth layer will spread inward from the edges forming the macrosteps [43,44].

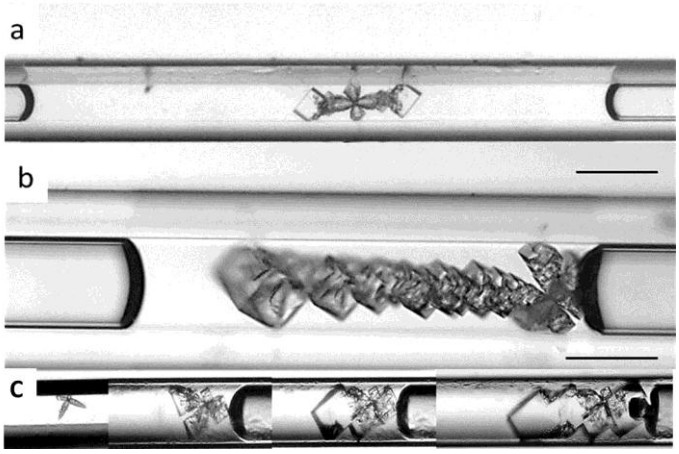

Figure 6: Spontaneous formation of Hopper crystals at S = 1.6 ± 0.2 in (a) 50 μm capillary: and, (b) 100 μm capillary. (c) Evolution of the growth of a Hopper crystal in the first 10 minutes (Scale=100μm)

However, since the nucleation rate depends very strongly on the concentration, such a rapid growth of the critical nucleus will lead to a very rapid decrease of the local supersaturation and consequently favors the formation of only a single skeletal crystal with a peculiar shape. It is noticed that the morphology of the Hopper crystals changes during the growth process, due to the gradual decrease of the ion concentration in the solution accompanying the formation of the crystals (figure 6c). At the late stages of growth regular cubic crystals start to form from the extremities of the Hopper crystal.

The Hopper crystals are growing in these experiments at a speed up to ten times that of the growth of a regular cubic crystal under the same conditions [27-45]; it is likely that such fast growth dynamics are accomplished with high supersaturations of the solution [45], hence provoking damage in porous materials. Indeed, the crystallization pressure that is responsible for the damage is known to depend strongly on the supersaturations reached [46,47].

3.2 Macroscale experiments

To see whether our conclusions from the capillaries also apply to real porous media, we compare the crystal morphologies at the late stages in microcapillaries with the NaCl crystals formed in experiments on porous sandstone. The surface of the latter was also treated as described in the experimental section to slow down the evaporation, prevent salt crystallization at the exterior of the stone and facilitate the formation of liquid pockets.

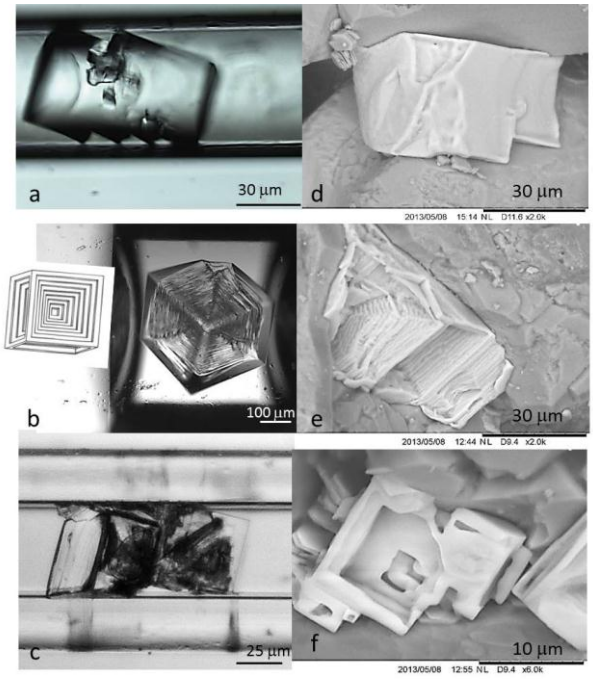

Figure 7: Comparison between NaCl crystals formed in capillaries after reaching our limit of supersolubility S~1.6 (a-c) and those obtained in the sandstone (d-f). All the experiments are performed at (T=22°C , RH~50%).

For that, the Mesne stone saturated with a NaCl solution (C_0=4.9M) is dried under the same conditions as the capillaries. Subsequently, the sample is fractured and the salt crystal morphology inside the stone is investigated by Scanning Electron Microscopy (SEM).

Figure 7 shows the remarkable similarities between the crystal structures formed in the stone and in the capillaries: in the stone also Hopper crystals have been formed. Observations on several samples show that these crystals are plentiful in some parts of the stone, while almost absent in others, suggesting that very concentrated residual fluid pockets had formed. Both these observations indicate that the liquid pockets in the stone behave similarly to the microcapillaries where high supersaturations were reached before crystallization starts.

This supersaturation seems to be sufficient to provoke damage. In fact, at S = 1.6 the crystallization pressure is about $\Delta P \sim 160$ MPa [16]. If we assume that only 15% of local volume fraction is filled with the salt, the related effective stress [48] in the sandstone will be $\sigma^* \sim 1{,}65$ MPa which is higher than the tensile strength of the Mesne sandstone (0.9 MPa). This is in a good agreement with the recent study on the damaging capacity of sodium chloride in stones, in which the formation of a crack in the drying front due to the development of enough effective stress was clearly shown [49].

4 Conclusion

In summary, we have demonstrated by controlled evaporation experiments of sodium chloride solutions, that the supersaturation achieved at the onset of spontaneous primary nucleation and growth is around 1.6 and remains independent of the size, shape and surface properties of the microcapillary. These results are consistent with expectations from classical nucleation theory. The metastability limit obtained here clearly shows that, contrary to what is commonly assumed for this salt [19,50], high concentrations can be reached before spontaneous crystal growth. This in turn leads to the formation of a Hopper crystal, which we also detected in analogous experiments conducted on real sandstone. Our findings therefore have far-reaching implications for the widespread consequences of salt crystallization [1-14] since the salt weathering of rocks, stones and monuments is related to the crystallization pressure which is directly dictated by the supersaturation.

References

[1] Pfann W.G. US Patent 3423189, (1969)

[2] Dutton R.L., Sharer J.M. Advanced technologies in biopharmaceuticals processing, (Blackwell publishing) (2007).

[3] Hunte C., von Jagow G., Schagger H., Membrane protein purification and crystallization; a practical guide (Academic press) (2003).

[4] Rengasamy P., Olsson K. A., Sodicity and soil structure. Aust. J. Soil. Res. (29) (1991), 935 - 952.

[5] Oelkers E.H., Gislason S.R., Matter J., Mineral carbonation of CO_2, Elements (4) (2008), 333-337.

[6] Muller N., Qi R., Mackie E., Pruess, K., Blunt, M. J., CO_2 injection impairment due to halite precipitation. Energy Proc. (1) (2009), 3507-3514.

[7] Peysson Y., Permeability alteration induced by drying of brines in porous media. Eur. Phys. J. Appl. Phys. (60) (2012), 24206.

[8] Fitzner B., Snethlage R., Einfluß der Porenradienverteilung auf das Verwitterungsverhalten asugewälter Sandsteine. Bautenschutz und Bausanierung. (3) (1982), 97–103

[9] Everett D.H., The thermodynamics of frost damage to porous solids, Trans. Faraday. Soc. (57) (1961), 1541-1551.

[10] Goudies A. S., Viles H. A., Salt Weathering Hazard (Wiley, London, (1997).

[11] Novak G.A., Colville A.A., Efflorescence mineral assemblages associated with crack and degraded residential concrete foundation in south California. Cem. Concr. Res. (1) (1989), 1-6.

[12] Scherer G.W., Stress from crystallization of salt, Cem. Concr. Res. (34) (2004), 1613-1624.

[13] Lubelli B., van Hees R. P. J., Huinink H. P., Groot C. J. W. P., Irreversible dilation of NaCl contaminated lime-cement mortar due to crystallization cycles, Cement and concrete research. (36) (2006), 678-687.

[14] Shahidzadeh-Bonn N., Desarnaud J., Bertrand F., Chateau X., Bonn D., Phys. Rev. E, (81) (2010), 066110.

[15] Viles H. A., Implication of future climate change for stone deterioration, Geo. Soc. Spec. Publ. (205) (1997), 407-418.

[16] Steiger M., Crystal growth in porous materials-1: The crystallization pressure of large crystals. J. Cryst. Growth. (282) (2005), 455.

[17] Flatt R. J., Salt damage in porous materials: how high supersaturations are generated? J. Cryst. Growth. (242) (2002), 435–454.

[18] Taber S., The growth of crystals under external pressure, American Journal of Science (41A) (1916), 532-557.

[19] Emmanuel S., Berkowitz B., Effect of pores size controlled solubility on reactive transport in heterogeneous rock, Geophys. Res. Lett. (34) (2010), L06404.

[20] Putnis A., Mauthe G., The effect of pore size on cementation in porous rocks, Geofluids (1) (2001), 37-41.

[21] Putnis A., Prieto M., Fernandez-Diaz L., Fluid supersaturation and crystallization in porous media, Geol. Mag. (132) (1995), 1-13.

[22] Aizenberg J., Black A.J., Whitesides G. M., Control of crystal nucleation by patterned self-assembled monolayers, Nature (398) (1999), 495-498.

[23] Diao Y., Harada T., Myerson A.S., Hatton T.A., Trout B.L.. The role of nanopore shape in surface induced crystallization. Nature Materials (10) (2011), 867-871.

[24] Shahidzadeh-Bonn N., Rafai S., Bonn D., Wegdam G., Salt crystallization during evaporation: Impact of interfacial properties, Langmuir (24) (2008), 8599-8605.

[25] Desarnaud J., Shahidzadeh-Bonn N., Salt crystal purification by deliquescence/crystallization cycling, Euro. Phys. Lett. (95) (2011), 48002.

[26] Page A.J., Sear R.P., Crystallization controlled by geometry of surface, J. Am. Chem. Soc. (131) (2009), 17550-17551.

[27] Shahidzadeh N., Desarnaud J., Damage in porous media: role of the kinetics of salt (re)crystallization, Eur. Phys. J. Appl. Phys. (60) (2012), 24205.

[28] Desarnaud J., Bertrand F., Shahidzadeh N., Impact of the kinetics of salt crystallization on stone damage during Rewetting/Drying and Humidity cycling, J. Appl. Mech. (80) (2013), 020039.

[29] Shahidzadeh-Bonn N., Azouni A., Coussot P., Effect of wetting properties on the kinetics of drying of porous media, J. Phys. Condens. Matter. (19) (2007), 112101.

[30] Camassel B., Sghaier N., Prat M., Nasrallah S.B., Evaporation in a capillary tube of square cross-section: application to ion transport, Chem. Eng. Sci. (60) (2005), 815-826.

[31] Chauvet F., Duru P., Geoffroy S., Prat M., The three periods of drying of a single square capillary tube, Phys. Rev. Lett. (18) (2009), 124502.

[32] Wong H., Morris S., Radke C. J., Three dimensional menisci in polygonal capillaries, J. Colloid. Interf. Sci. (48) (1991), 317.

[33] Lubelli B., van Hees R.P.J., Groot C., Gunneweg J., Risks of the use of water repellent and consolidating treatments on salt contaminated masonry: the case of a wind mill in the Netherlands, Restoration of building and monument (13), 319-330.

[34] Pavlík Z., Michálek P., Pavlíková M., Kopecká I., Maxová I., Černý R., Water and salt transport and storage properties of Msené sandstone, Construction and Building Materials (22) (2008), 1736-1748.

[35] Kestin J., Khalifa E., Correia R. J., Tables of the dynamics and kinematic viscosity of aqueous NaCl solutions in the temperature range 20-150ºC and the pressure range 0.1-35 MPa. J. Phys. Chem. Ref. Data. (10) (1981), 71-87.

[36] Mullin J. W., Crystallization, (Butterwords-Heinemann, 4th edition), (2001).

[37] Bird R. B., Stuwart W. E., Lightfoot E. N., Transport phenomena (Wiley, New York), (1960)

[38] Robinson R. A., The Vapour Pressures of Solutions of Potassium Chloride and Sodium Chloride, Trans. Roy. Soc. New Zealand. (122) (1945), 203-217.

[39] Valeriani C., Sanz E., Frenkel D., Rate of Homogeneous Nucleation in Molten NaCl, J.Chem.Phys. (122) (2005), 194501 1-6.

[40] Sear R., Nucleation: Theory and Applications to Protein Solutions and Colloidal Suspensions, J. Phys. Condens. Matter. (19) (2007), 033101 1-28.

[41] Mucha M., Jungwirth P., Salt Crystallization from an Evaporating Aqueous Solution by Molecular Dynamics Simulations, J. Phys. Chem. B (107) (2003), 8271-8274.

[42] Chakraborty D., Patey G.N., How Crystals Nucleate and Grow in Aqueous NaCl Solution. J. Phys. Chem.Lett. (4) (2013), 573-578.

[43] Sunagawa I., Growth and morphology of crystals. Forma (14) (1999), 147-166.

[44] Kuroda T., Irisawa T., Ookawa A. Growth of a polyhedral crystal from solution and its morphological stability, J. Cryst. Growth (42) (1972), 41-46.

[45] Al-Jibbouri S., Ulrich J., The growth and dissolution of sodium chloride in a fluidized bed crystallizer, J. Cryst. Growth (2002) (234), 237.

[46] Correns C. W., Growth and dissolution of crystals under linear pressure, Discussions of the Faraday Soc. (5) (1949), 267–271.

[47] Steiger M., Crystal Growth in Porous Materials II: Influence of Crystal Size on the Crystallization Pressure, J. Cryst. Growth (282) (2005), 470-481.

[48] Espinosa-Marzal R., Hamilton A., McNall M., Whitaker K., Scherer G.W., The Chemomechanics of Crystallization During Rewetting of Limestone Impregnated with Sodium Sulfate, J. Mater. Res. (26) (2011), 1472-1481.

[49] Derluyn H., Mooneen P., Carmeliet J., Deformation and Damage due to Drying Induced Salt Crystallization in Porous Limestone. J. Mech. Phys. Solids (63) (2014), 242-255.

[50] Bouzid M., Mercury L., Lassin A., Matray J. M., Salt Precipitation and Trapped Liquid Cavitation in Micrometric Capillary Tubes. J. Colloid and Interf. Sci. (360) (2011), 768-776.